DETECTION OF VISUAL DOUBLE STARS WITH GAIA

V.V. Makarov, F. Arenou
SAG-CUO-80
Meudon, Copenhagen, November 24, 2000

Abstract

Visual double stars will constitute a considerable fraction of all observable stars with GAIA. They pose certain problems for the on-board detection algorithm, which should be able to resolve double stars into components down to separations of 0.1 arcsec in order to have both components safely contained within a patch of standard size (6 pixels wide). An attempt is made at estimating the performance of an optimal, or minimum variance bound estimator in resolving double stars, and a practical realization of duplicity detection is discussed. This is used to estimate for which double stars the above requirement will be met. Stars brighter than 19.5 mag with separations larger than 0.12 arcsec and $\Delta G < 3$ mag will often be resolved at the detection stage at ASM, and a double patch (12 pixels wide), or a patch of double size, should be taken at the astrometric field, for proper on-ground treatment of these objects. Stars with separations smaller than 0.1 arcsec will sometimes not be resolved at ASM, but the star image will hardly be impaired by cutting off part of the signal outside the patch. The prospects of accurate astrometry of such systems in the following on-ground processing are fair. If a 'good' detection technique is implemented for ASM, the only concern is about pairs of ΔG greater than 4 to 5 mag with faint secondary components, which at some specific separations will not be detected as doubles, and therefore irreparably damaged by patching.

1. VISUAL DOUBLE STARS OBSERVABLE WITH GAIA

Resolved double stars are important with regard to the GAIA mission objectives for two reasons. Firstly, obtaining separate and very accurate astrometric and photometric data on components of physical binary and multiple stars will allow to advance in such fields of stellar and Galactic astrophysics as mechanisms of binary system formation, dynamic evolution of multiple systems and the initial mass function of various Galactic populations. Secondly, achieving the required accuracy in photometry and astrometry would not be possible for many stars if their duplicity is not detected from the GAIA observations, and therefore neglected in the data processing.

In the range of observed separations 5 to 50 AU, for example, the ratio of binary/triple systems to single stars is about 0.2 for nearby G dwarfs, 0.4 for the Hyades cluster (age 600 Myr) and 0.7 for T Tauri stars (Patience et al. 1998). In an open cluster like the Hyades at a distance of 500 pc about 30% of all stars will turn out to be visual binaries at separations 0.01 to 0.1 arcsec, which will hamper the final results unless detected and properly treated as a separate class of objects. Considering all presently observable separations, including spectroscopic binaries, only 30% of solar type stars appear to be truly single (Duquennoy & Mayor 1991), and practically nothing is known of the frequency of very low-mass companions ($M_2 < 0.01 M_\odot$).

2. DETECTABILITY OF DOUBLE STAR COMPONENTS

Let $p(x, y)$ be the point-spread function (psf) of a given ASM1 CCD chip. The expected image of a star component is

$$I(x, y) = A_1 p(x - x_1, y - y_1), \tag{1}$$

where (x_1, y_1) is the position of the component, and A_1 is its amplitude expressed in photoelectrons, which depends on the magnitude. The expected image $J(x, y)$ of a secondary component at (x_2, y_2) is expressed similarly. The observed image of this double star is

$$O(x,y) = C(x,y) + b + n = I(x,y) + J(x,y) + b + \text{noise}, \tag{2}$$

where b is the local background, assumed hereafter to be constant within the processed part of the image, and n is additive noise. The sampled image on the CCD can be represented by a vector O_i, $i = 1, \ldots, n$, where n is the number of discrete sample points.

The technique of optimal linear filtering, described in SAG-LL-29 (Lindegren 2000), has the practical advantage of being able to predict, which images (or structures) are theoretically detectable with a given set of instrument specifications. It can easily be extended onto the case of double stars. For any given image C_i there is an *optimal* linear filter w_i that yields the maximal signal to noise ratio (SNR) in the filtered image. In this case, we consider an *ideal*, i.e., optimal for double star detection, algorithm, which subtracts from O_i the expected image of the primary component, and filtres the residual image in the optimal way in order to detect the secondary component. The optimal filter in this case is, explicitly,

$$w_i = K \frac{J_i}{C_i + b + r^2}, \tag{3}$$

where r is the rms readout noise per sample, and K is the constant normalizing w_i to unity area. The maximum SNR for the secondary component is

$$\mathrm{SNR}_J = \left[\sum_i \frac{J_i^2}{C_i + b + r^2} \right]^{\frac{1}{2}}. \tag{4}$$

The value of the above formula is that it gives the maximal theoretically achievable SNR in detection of the secondary component of a double star. Thus, setting a certain limit on SNR, for example 7, provides the absolute lower bound of detectability for a given instrument. No algorithm can surpass this limit, because beyond this bound, the signal from the secondary component is too weak compared to the noise in the combined image.

The variety of existing algorithms may be considered as approximations to the optimal algorithm of subtracting the expected image of one component and detecting the other. In any case, the combined signal must be split between the two components. If no *a priori* information is available for a given double system, any practical implementation of a detection algorithm will face the formidable task of estimating at least 6 unknowns, inter-related in a nonlinear way through the psf (4 coordinates and 2 magnitudes). Therefore, a detection algorithm will quite likely be iterative, and hence quite slow. In the Tycho-2 double star processing, for example, a rather straightforward iterative algorithm was used (Fabricius & Makarov 2000, Høg et al. 2000). One iteration included subtraction of one component with the previously estimated parameters, and a full astrometric and photometric estimation of the other from the residual image.

The basic flaw of Eq. 4 is the assumption, that the expected image of the primary component can be subtracted cleanly from the observed image. This gives too optimistic estimates at very close separations, and even non-zero SNR at null separation, whereas at null separation, the combined image is indistinguishable from a single star image of combined amplitude. The upper bound estimate can be improved in the following way

$$\mathrm{SNR}_J = \min \left\{ \begin{array}{l} \left[\sum_i \frac{J_i^2}{C_i+b+r^2} \right]^{\frac{1}{2}} \\ \left[\sum_i \frac{(C_i - (1+A_2/A_1) I_i)^2}{C_i+b+r^2} \right]^{\frac{1}{2}} \end{array} \right. \tag{5}$$

Eq. 5 is more realistic, because it gives a zero SNR for null separations. It implies that a single star image of a combined amplitude $(A_1 + A_2)$ is subtracted at the position of the primary component, which is relevant at close separations. Generally, it is a good assumption for pairs of large ΔG and small separations, because nearly all the signal in such binaries is centred on the primary component. However, when the components are similar in magnitude, this approximation gives far too optimistic results. What is practically important, is whether a certain realization of the detection algorithm is able to detect a statistically significant residual signal in the first iteration, assuming a single star image. At least in the ASM1, if the on-board programme fails to find any evidence of a binary component, it will stop further attempts to resolve the object. Astrometric estimation in the first iteration is more likely to produce the position of the photocentre, rather than the position of the primary. Thus, a more plausible algorithm includes subtraction of the expected image at the position of the photocentre. The improved, and final model is

$$\mathrm{SNR}_J = \min \left\{ \begin{array}{l} \left[\sum_i \frac{J_i^2}{C_i+b+r^2} \right]^{\frac{1}{2}} \\ \left[\sum_i \frac{(C_i - H_i)^2}{C_i+b+r^2} \right]^{\frac{1}{2}} \end{array} \right. \tag{6}$$

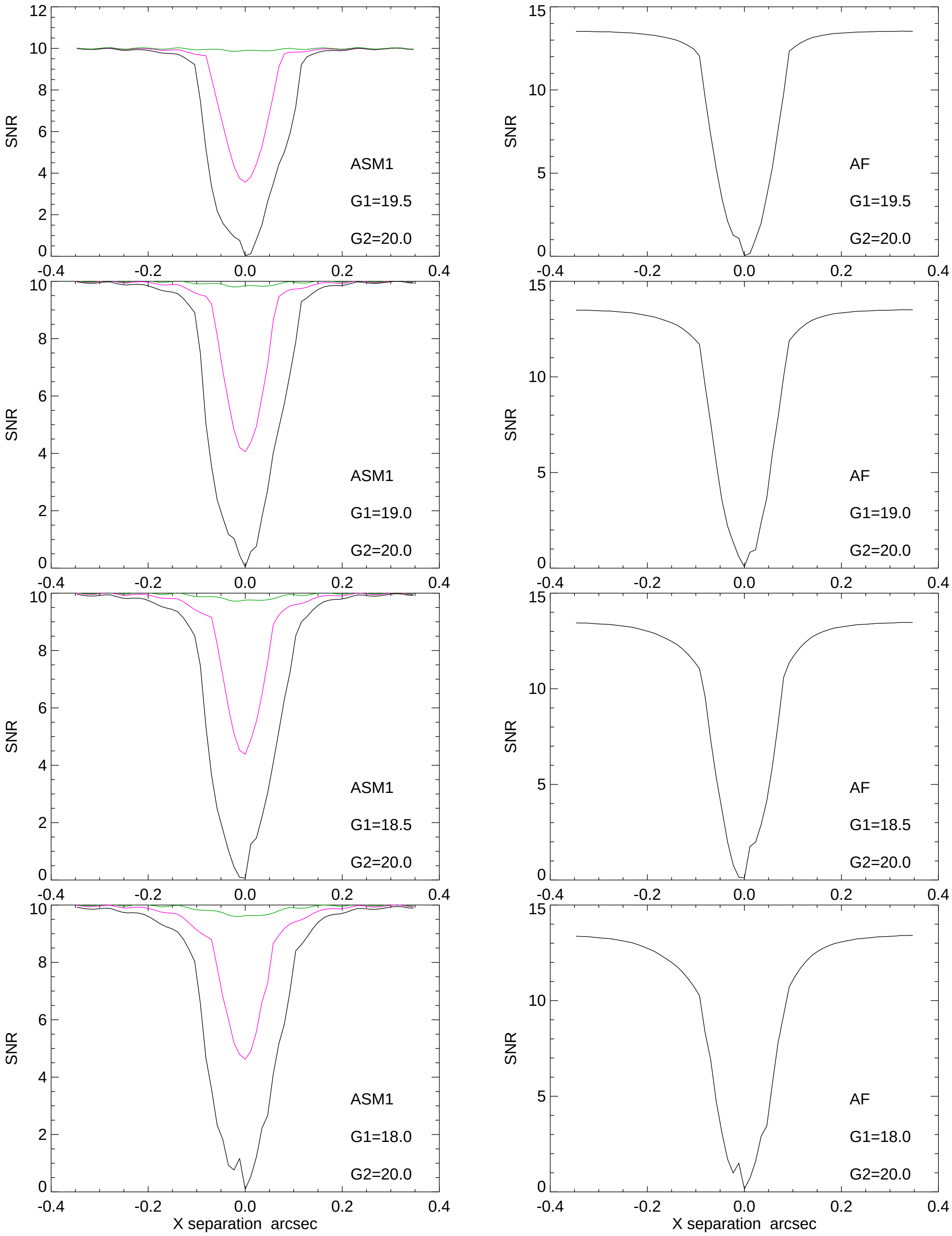

Figure 1. Computed SNR for a secondary component of magnitude $G = 20.0$ at the ASM1 (left column) and AF (right) with a primary of four different magnitudes, as function of positional separation. A black line (lower curve) for the ASM1 plots corresponds to a null separation in the vertical (across scan) direction, a red line (middle) to a vertical separation of 1 sample = 0.223 arcsec, and a green line (upper) to a vertical separation of 2 samples. For the AF, only along-scan separations are given. The psf for a star with $V - I = 1.0$ mag, field point 13 for ASM1 and field point 1 for AF, are adopted.

where

$$H(x, y) = (A_1 + A_2)p(x - x_p, y - y_p), \tag{7}$$

Table 1. Lower bounds of angular separation in arcsec, at which a safe detection of binarity is achieved with a SNR of 10. The limit of 10 may seem excessively high, but it is justified in Sect. 4. The basic parameters of the GAIA astrometric instruments are assumed, i.e., for ASM1, $r = 10.9$ electrons per sample of 2×2 pixels per CCD, $b = 2$ electrons, and for AF $r = 6$ and $b = 5$ per one sample of 1×6 pixels. Either component has $V - I = 1.0$ mag, and the primary component is centred on a sample. PSF for field point 13 is used for ASM1, and field point 1 for AF. A '$-$' denotes no detection within 0.35 arcsec of the primary component. A null vertical (across-scan) separation is assumed.

	ASM1							AF						
	$G_2 = 20.0$	19.5	19.0	18.5	18.0	17.5	17.0	$G_2 = 20.0$	19.5	19.0	18.5	18.0	17.5	17.0
$G_1 = 20.0$	0.35							0.09						
19.5	-	0.09						0.08	0.07					
19.0	-	0.09	0.08					0.08	0.07	0.06				
18.5	-	0.09	0.08	0.07				0.08	0.07	0.06	0.05			
18.0	-	0.09	0.08	0.07	0.06			0.09	0.07	0.06	0.05	0.05		
17.5	-	0.10	0.08	0.07	0.06	0.06		0.11	0.08	0.06	0.05	0.05	0.04	
17.0	-	0.10	0.09	0.07	0.06	0.05	0.05	0.13	0.08	0.06	0.05	0.05	0.04	0.04
16.5	-	0.12	0.09	0.07	0.06	0.05	0.05	0.16	0.09	0.07	0.06	0.05	0.04	0.03
16.0	-	0.13	0.10	0.08	0.06	0.05	0.04	0.19	0.11	0.08	0.06	0.05	0.04	0.03
15.5	-	0.17	0.11	0.08	0.07	0.06	0.05	0.22	0.13	0.09	0.07	0.05	0.04	0.04
15.0	-	0.19	0.11	0.09	0.07	0.06	0.05	0.27	0.16	0.10	0.08	0.06	0.04	0.04
14.5	-	0.23	0.14	0.09	0.08	0.07	0.05	0.32	0.19	0.12	0.07	0.05	0.05	0.04
14.0	-	0.27	0.16	0.11	0.07	0.07	0.06	-	0.22	0.15	0.09	0.05	0.04	0.02
13.5	-	0.33	0.19	0.12	0.09	0.06	0.03	-	0.26	0.17	0.11	0.06	0.03	0.02

and (x_p, y_p) is the position of the photocentre, determined as the weighted mean of the two component positions.

Fig. 1 depicts expected SNR of the secondary component computed by Eq. 6 for components of different magnitudes. The psf for the field point 13 was assumed for ASM1, and the field point 1 for AF. Either component has $V - I = 1.0$ mag, which is not realistic. We will discuss the problems that arises from the colour ambiguity at the detection stage in the following section. The wobbles of the curves at low SNR are likely caused by a pixel discretization noise in our computations.

Table 1 gives the minimum separations detectable at ASM1 and AF, for different magnitudes of the primary and the secondary, with a SNR$= 10$. The primary component is assumed to be centred on the central sample. Computations show that a decentering of the primary component does not change the numbers so much. The minimum separation is quite flat at ΔG below 2.5 mag. Astrophysically more important cases of large ΔG depend on the magnitude of the secondary. Finally, the performance of ASM1 at resolving double stars is only slightly ($\approx 20\%$) worse than that of AF. This confirms that the sizes of samples and pixels are close to optimal. The difference between ASM1 and AF is most noticeable at faint magnitudes, where the larger read-noise for the former becomes critical. The ASM3 instrument, which has a lower read-noise of 6 e^-, will be very similar to AF at resolving faint pairs.

A drastic improvement of performance at AF can be achieved by stacking the 16 images from one transit. The combined resolution capability can be computed by Eq. 6 for a 4 times smaller limiting SNR, e.g., 2.5. This is, however, of only academic interest for stars wider than ≈ 0.1 arsec if they are not resolved at ASM. The patch of 0.223×0.839 mas^2 from AF will be centred on the photocentre of the system. A certain part of the signal will be lost for the on-ground astrometric and photometric analysis, depending on the separation and ΔG. Fig. 2 represents the total signal loss for pairs of different ΔG due to the cutting off part of the image by a patch of 6 samples wide, and the loss for the secondary (fainter) component. Here we assume that the astrometric estimation, which comes first in the detection process at ASM1, provides the photocentre for an unresolved pair of stars, that is the weighted mean position. It is clear, that the patching technique will not damage the primary when $\Delta G > 2$ mag, no matter what the separation is. Both components will be irreparably damaged if the separation is larger than ≈ 0.12 arcsec, $\Delta G < 2$ and the duplicity is not detected. But the secondary is the major looser, being irrevocably damaged for the future on-ground analysis at separations 0.08 to 0.15 arcsec and larger, depending on ΔG. The most interesting doubles of very large ΔG will be the most difficult to handle. For instance, as follows from a comparison of Table 1 and Fig. 2, secondaries fainter than $G = 18.5$ in pairs of $\Delta G > 4.5$ and at separations just above the minimum obtainable limit, will be severely trimmed by patches. Of course, at other scan directions, when the projected separation is smaller, both components will safely be within one patch, but such observations will not contribute to the on-ground duplicity analysis, because the AF patch does not have sufficient across-scan resolving power.

On the contrary, when a double is detected at ASM, some options could be considered to avoid any impairment of the basic observation data in the main field. A command could be generated for AF to read and transmit a larger patch, for example. Separate patches could be taken for components of very large ΔG at wider separations. Practical implementation of such contingencies will depend much on the performance characteristics of the

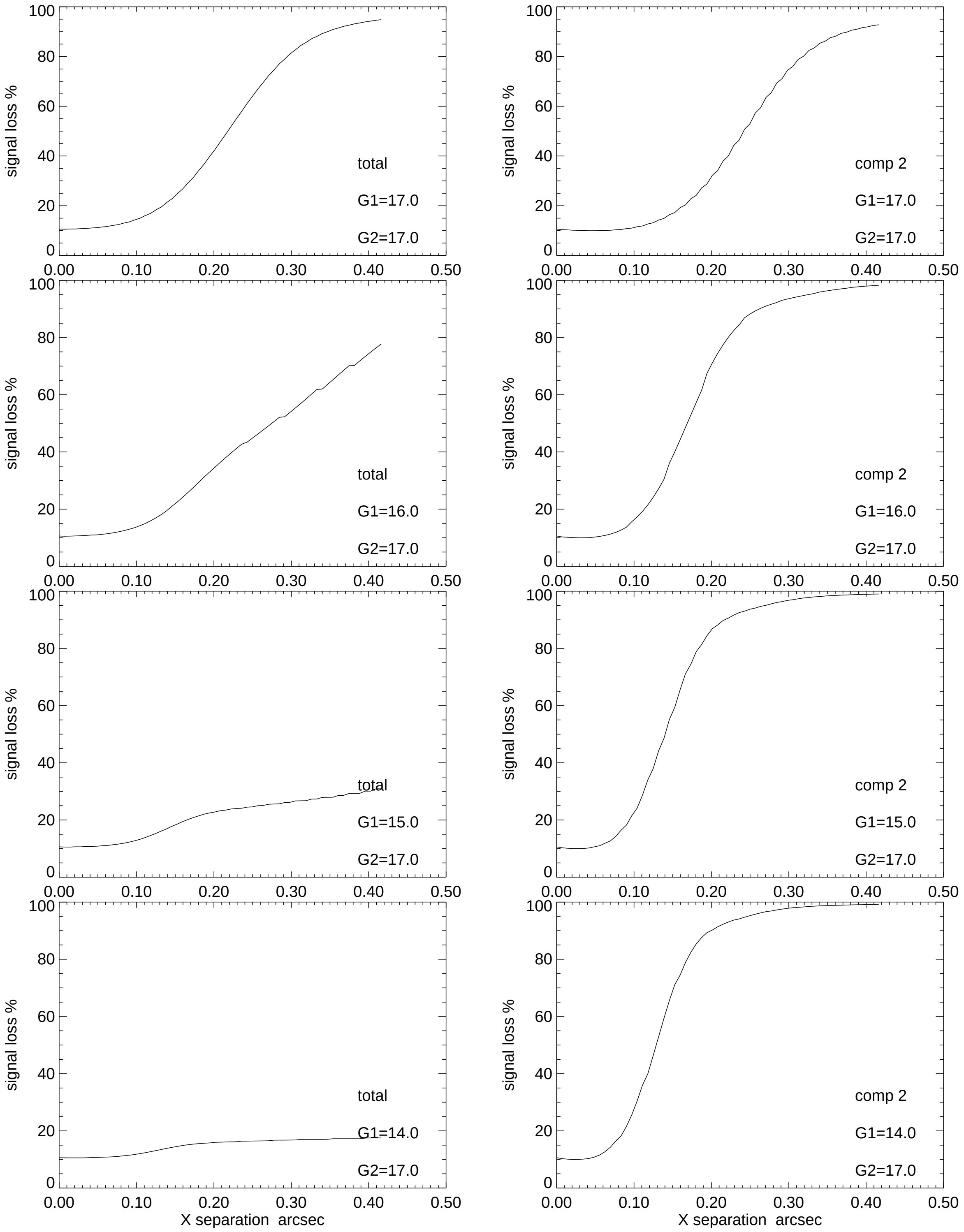

Figure 2. The fraction of signal that is lost for an AF patch of 6 samples wide, centred on a photocentre of a double star. The total signal loss for the two components is shown in the left column of plots, and the signal loss for the secondary component in the right. The photocentre is computed as the weighted mean of the two component positions. A null vertical separation is assumed. The psf for a star with $V - I = 1.0$ *mag at field point 13 is adopted for both components.*

detection method, e.g., to what precision it will be able to estimate the separation.

3. THE COLOUR AMBIGUITY

When a star is detected at ASM, nothing is known about its colour. The cleaning algorithm of double star detection, outlined in the previous section, will have to start with a certain assumption of a 'standard' colour and the psf that corresponds to it. The actual star image will often be broader if the star is redder than the standard colour, and narrower if it is bluer. The first subtraction of the expected 'standard' star image at the estimated position, even for a genuinely single star, may result in a residual pattern similar to a duplicity signature.

More specifically, if a star is redder than the standard, the residual image will consist of a central dip surrounded by a bright (positive) ring. A similar pattern is expected when a single star image is subtracted from the observed image of a double star. Certainly, the shape of the residual image will not be the same, especially for a pair of a large ΔG and separation, but close companions of similar magnitudes will perhaps be harder to tell from a single red star.

We will try to find out now, under which conditions such a confusion may take place. Suppose, a single star image is tested with a duplicity detection filter that derives from the model (6)

$$w_i = \frac{C_i - H_i}{C_i + b + r^2}, \tag{8}$$

assuming, for a start, two components of equal magnitude at a given separation. It is assumed again, that the total number of electrons in the image is correctly estimated by, e.g., an aperture photometry method. The signal resulting from the convolution of the filter function with the residual image $R - H$ can be explicitly computed as a function of separation, adopting a certain $V - I$ colour as standard for H. R is an image of a single star in this experiment, but of a redder colour than H.

Fig. 3 shows the resulting SNR at the position of the red single star image R, with colours $V - I = +5$ and $+3$ mag. The standard star colour is assumed to be $+1.0$. The star is centred on the central sample. Adopting again a limit of 10 on SNR, we conclude that a star of $V - I = +5$ may be spuriously detected as double and consisting of two equally bright components if brighter than about 16.5 mag. The range of 'confusion' separations is sharply limited to within about 0.13 arcsec. This sudden drop in SNR is explained by geometrical characteristics of the undersampled star image and the filter. Most of the signal from the star is distributed over only three samples, the central sample dominating the rest. A similar shape is produced by a double star as long as the separation is smaller than about 2 samples, where a dip appears in the central sample, and therefore a mismatch between the filter and the observed image. A star of $V - I = +3$ exhibits the same cut-off separation, but a lower SNR of detection, so that an SNR of 10 may be obtained for stars brighter than about $G = 16$. If the star is centred on the boundary between two adjacent samples, the SNR becomes significantly smaller for the same G, indicating a lesser degree of confusion, and putting the limiting magnitude approximately 1.5 mag brighter, but the cut-off separation stays put.

This experiment proves that a red sufficiently bright single star may be taken for a double of a small separation. But it does not imply that these two cases can not be distinguished by linear filtering. Consider, for example, a star of $V - I = +5$ and $G = 16.5$, assumed to be a double comprising two components of standard colour and $G = 17.25$, yielding together the same number of photoelectrons. As follows from the third plot from top in the left column of Fig. 3, the SNR in the filtered residual image will be just above 10, enough to trigger a duplicity detection. However, if the object was indeed a double star of these parameters, the resulting SNR with the same filter would be about 50. This is to be expected, because the filter is *optimal* for this exact configuration of components, but not for a single red star. Although the residual patterns are similar, they are significantly different in shape. We could construct an *optimal* filter for a single star of a given colour, exploiting the possibility to estimate the colour from the shape of the observed image.

A detection procedure may therefore be seen, in principle, as a statistical testing of various hypotheses about the object in question. The range of hypotheses may include objects like single stars of various colours, double stars of various separations and ΔG (and colour), non-stellar objects, etc. For each of these objects, an optimal detection filter can be constructed, and decision may be taken on the type of the object depending on the resulting SNR. It is quite clear that this way is not practical, because the range of hypotheses is infinite. Some of the uncertainties will be eliminated in the on-ground reductions, for example, the colour of the object will be accurately determined from photometric observations. A much simpler algorithm is required for the on-board detection. It appears, that the possibility of confusion between a single red star and a double star of $\Delta G = 0$ and separation less than 0.13 arcsec is of no practical importance, and does not require any special on-board action, because such a double fits well into the normal patch (cf. top plots in Fig. 2). However, our computations show, that double stars of non-equal components will be increasingly hard to distinguish from single red stars, because the cut-off separation very rapidly increases with growing ΔG.

A practical solution could be to always take a larger patch at AF if a duplicity threshold is exceeded. The relative burden for the volume of data transmission will be small, because only very bright and red stars will trigger the duplicity detection.

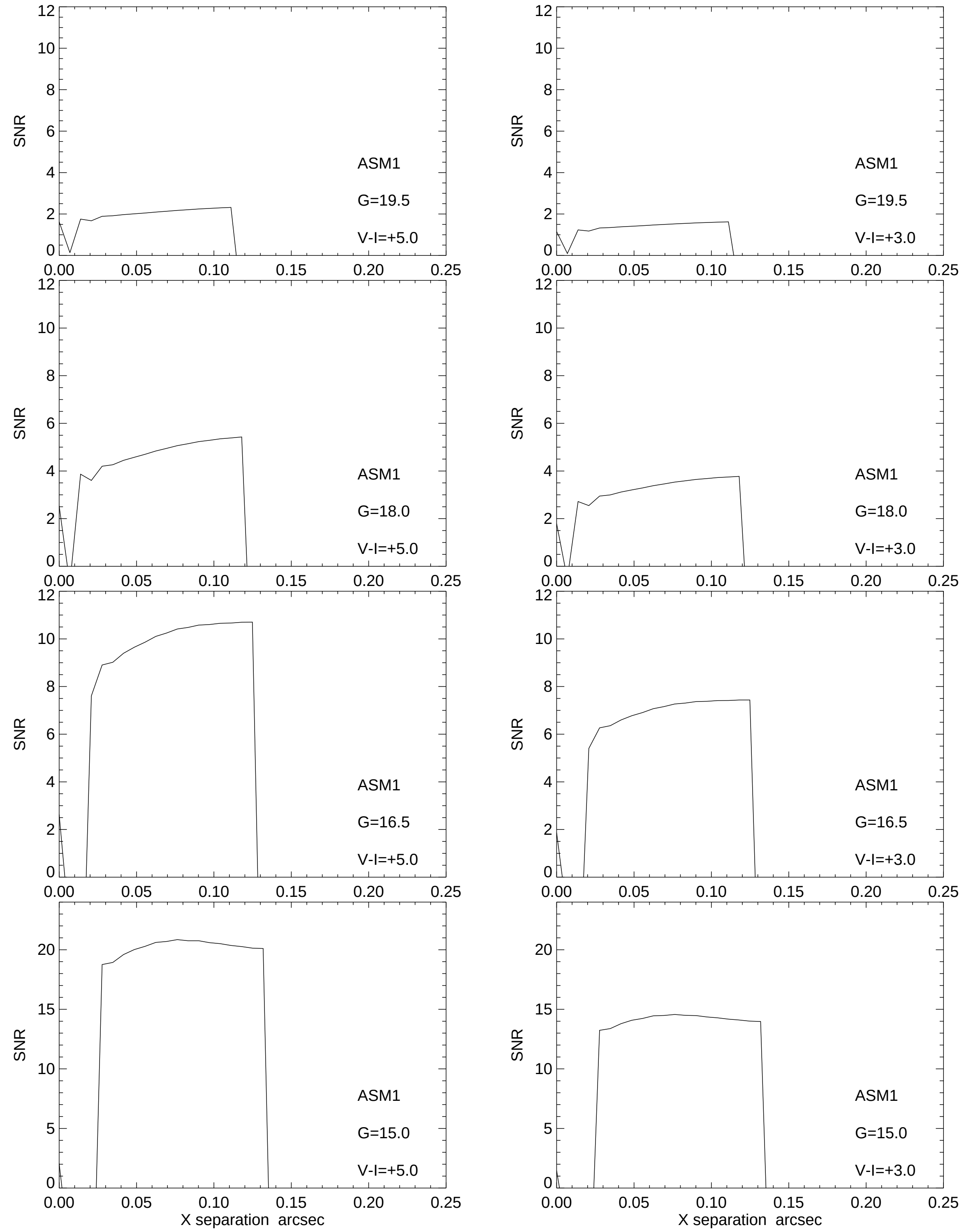

Figure 3. Computed SNR at ASM1 for a single star of $V-I=+5$ (left column) and $+3.0$ mag (right), as obtained with an optimal filter for detection of a double star with components of equal brightness. The star image is centred on the central sample. The psf for a star with $V-I=1.0$ mag at field point 13 is adopted as a standard image (see text).

4. OPTIMAL FILTERS, THE CRAMÉR-RAO LOWER BOUND AND PROBABILITIES

The Cramér-Rao lower bound (also called the minimum variance bound, MVB) is an important characteristic of a given estimator and probability distribution. It represents the minimum obtainable variance of a given estimate. In some particular applications, the lower bound has analytic expressions (Kendall & Stuart 1973). Since the optimal filter (Eq. 3) is designed to yield the largest possible SNR in the filtered image, the variance of the (photometric) estimator should be expected to equal the Cramér-Rao lower bound for each element of the image, including the true location of the star. That this is really the case, occurs from adapting Eq. 11 in (Zaccheo et al. 1995) to our case of non-zero Gaussian noise, and neglecting the bias term

$$\mathrm{CR}_k^2 = \sum_i w_{i+k}^2 (C_i + b + r^2), \tag{9}$$

where CR_k^2 is the lower bound variance at sample k. It is noted that Eq. 9 gives the lower bound for any photometric estimator, as long as it is realised through a linear filter. In our case, a photometric estimator may concern the amplitude of the secondary component A_2. For example, model (4) finds a comprehensible photometric interpretation. According to Kendall & Stuart (Vol. 2, Sect. 17.17), t is a MVB estimator of $\tau(\theta)$, if the condition

$$\frac{\partial \log L}{\partial \theta} = f(\theta)[t - \tau(\theta)] \tag{10}$$

is satisfied, where L is the likelihood function, f is a function of θ, but not of the observations. To facilitate the computation of of L, we assume that the zero-point of the observed values is r^2, as is done in (ESA-SCI(2000)4 2000). The read-noise may be considered now as approximately Poissonian, which is a good approximation for all but very faint objects. It is equivalent to introducing a constant background

$$B = b + r^2. \tag{11}$$

The likelihood function is then

$$L = \prod_i \frac{(C_i + B)^{O_i}}{O_i!} \exp(-C_i - B). \tag{12}$$

Since

$$\frac{\partial \log L}{\partial A_2} = \frac{1}{A_2} \sum \frac{J_i}{C_i + B} (O_i - C_i - B), \tag{13}$$

it becomes clear that $\sum w_i (O_i - I_i - B)$ is a MVB estimator of $\tau(A_2) = \sum w_i J_i$ provided w_i is the optimal filter (3).

But how to construct an optimal filter if we do not know the type of detected objects? Even the model (6), which we called the most realistic, is a long way from practical realization, because the noiseless combined image C_i is not known. [If it was known, we would not need to detect anything.] A natural option is to substitute C_i in Eq. 8 with the observed image $O_i - b$. The filter is now

$$w_i = \frac{O_i - b - H_i}{O_i + r^2}, \tag{14}$$

and the estimator takes the form

$$t = \sum \frac{(O_i - b - H_i)^2}{O_i + r^2}. \tag{15}$$

For a large sample (i.e., sufficiently bright star) one may use

$$\mathrm{var}[t] \approx \sum \left[\frac{\partial t}{\partial O_i}\right]^2 \mathrm{var}[O_i] = \sum \frac{(C_i - H_i)^2 (C_i + 2b + 2r^2 + H_i)^2}{(C_i + b + r^2)^3}. \tag{16}$$

For small separations $C_i \approx H_i$, hence $\mathrm{SNR}_O \approx 0.5\,\mathrm{SNR}_J$, where SNR_J is computed by Eq. 6. The SNR values given in Fig. 1 should be roughly divided by 2 if we want to estimate the performance of this estimator. Consequently, Table 1 gives the resolution limits at a limiting SNR$\approx$ 5 for this practical way of duplicity detection.

The recipe of this tentative method is

- Estimate the position of the detected object by an astrometric estimator;
- Estimate the total number of photoelectrons in the image by, e.g., an aperture photometry method;
- Construct the filter (14), compute the estimator t and compare it with the threshold value.

The actual performance of this estimator will be further aggravated by the errors in the preceeding astrometric and photometric estimations. It is also clear that the estimator thus constructed is biased, and will typically provide positive values even for perfectly single stars. The threshold values of SNR should include the bias. These issues would be best addressed by direct Monte-Carlo simulations.

REFERENCES

Duquennoy A., Mayor M., 1991, A&A 248, 485

ESA-SCI(2000)4, GAIA, Concept and Technology Study Report, 2000

Fabricius C., Makarov V.V., 2000, A&A 356, 141

Høg E., et al., 2000, A&A 357, 367

Kendall M.G., Stuart A., 1973, The Advanced Theory of Statistics, Vol. 2, New York

Lindegren L., 2000, SAG-LL-29

Patience J., et al., 1998, AJ 115, 1972

Zaccheo T.S., Gonsalves R.A., Ebstein S.M., 2000, ApJ 439, L43